EFFICIENCY AND COHERENCE IMPROVEMENT FOR MULTI APERTURE INTERFEROGRAM (MAI)

Hyung-Sup Jung*, Chang-Wook Lee*, Wook-Park*, Sang-Wan Kim**, Van Trung Nguyen*, Joong-Sun Won*

*Department of Earth System Sciences, Yonsei University 134 Sinchon-dong, Seodaemun-gu, Seoul 120-749, Korea.
geohyung@yonsei.ac.kr
** Department of Geoinformation Engineering, Sejong University, 98 Gunja-Dong, Gwangjin-Gu, Seoul 143-747, Korea.

ABSTRACT ... While conventional interferometric SAR (InSAR) technique is an excellent tool for displacement observation, it is only sensitive to one-dimensional deformation along the satellite's line-of-sight (LOS). Recently, a multiple aperture interferogram (MAI) technique has been developed to overcome this drawback. This method successfully extracted along-track displacements from InSAR data, based on split-beam InSAR processing, to create forward- and backward- looking interferograms, and was superior to along-track displacements derived by pixel-offset algorithm. This method is useful to measure along-track displacements. However, it does not only decrease the coherence of MAI because three co-registration and resampling procedures are required for producing MAI, but also is confined to a suitable interferometric pair of SAR images having zero Doppler centroid. In this paper, we propose an efficient and robust method to generate MAI from interferometric pair having non-zero Doppler centroid. The proposed method efficiently improves the coherence of MAI, because the co-registration of forward- and backward- single look complex (SLC) images is carried out by time shift property of Fourier transform without resampling procedure. It also successfully removes azimuth flat earth and topographic phases caused by the effect of non-zero Doppler centroid. We tested the proposed method using ERS images of the Mw 7.1 1999 California, Hector Mine Earthquake. The result shows that the proposed method improved the coherence of MAI and generalized MAI processing algorithm.

KEY WORDS: Multi aperture interferogram (MAI), SAR, ERS, along-track displacements

1. INTRODUCTION

Differential synthetic aperture radar interferometry (DInSAR) is a technique that has been successfully used for estimating large-scale surface deformation. During past twenty years, DInSAR technique has estimated crustal movements at the surface of the earth, which provide vital clues about the mechanism of the events like earthquakes and landslides. A disadvantage of DInSAR technique is just to estimate one-dimensional deformation along the satellite's LOS (line of sight) direction. To overcome this drawback, many researchers have studied on the incorporation of multiple radar passes (Fialko, 2004; Froger et al., 2004). Although these solutions are very useful for measuring the ground range and vertical components of deformation, the along-track deformation component is not estimated from data acquired by currently operating satellites.

The amplitude pixel offset method was used for measuring the along-track deformation by using cross correlation of two or more amplitude images. Although this method has very reduced sensitivity, it was in fairly wide use (Fialko et al., 2005; Jonsson et al., 2002). Recently, Bechor and Zebker (2006) proposed a new method to extract along-track displacements from InSAR data, based on split-beam InSAR processing, to create forward- and backward- looking interferograms. It was superior to amplitude pixel offset approach. It was implemented using conventional InSAR software (range-Doppler processing), steering the beam by modifying the Doppler centroid, and limiting the integration time to the appropriate interval (Bechor and Zebker, 2006). The approach is very simple and easy, but decreases coherence of MAI because of requiring three co-registration and resampling procedures. It also ignores the azimuth flat earth and topographic phases caused by the effect of non-zero Doppler centroid.

We propose an efficient and robust method to generate multiple aperture InSAR (MAI). In the proposed method, the co-registration of forward- and backward- looking interferograms is accomplished in azimuth compression step by the same range migration correction for range co-registration and the time shift property of Fourier transform for azimuth co-registration. This method generates MAI from forward- and backward- looking differential Interferograms to remove the effect of non-zero Doppler centroid. This method does not only improve the coherence of MAI, but also extends MAI processing to the image with non-zero Doppler.

The remainder of the paper is organized as follows. Section 2 explains the method that measures the along-track component of deformation using sub-aperture processing in detail. In section 3, the result of application using ERS images of the Mw 7.1 1999 California, Hector Mine Earthquake is presented. Finally, conclusions are provided in Section 4.

2. ALGORITHM

The MAI generation algorithm proposed by Bechor and Zebker (2006) are improved by decreasing the resampling step and removing the azimuth flat earth and topographic phases. The algorithm for MAI is implemented in azimuth compression step of range-Doppler processing using the same range migration correction for co-registration of range direction and the time shift property of Fourier transform for co-registration of azimuth direction.

2.1 MAI phase definition

For a displacement x in the along track direction, the MAI phase ϕ_{MAI} is (Bechor and Zebker, 2006):

$$\phi_{MAI} = \frac{4\pi}{l} nx, \tag{1}$$

where λ is radar wavelength, l is the effective antenna length, and n denotes a normalized squint changing the aperture width.

2.2 Azimuth compression for MAI

Consider the master and slave images with Doppler centroids of f_{DC1} and f_{DC2} as depicted in Figure 1. For efficiently generating MAI, it is important to reconcile Doppler centroid of master image with that of slave image, and then the Doppler centroid of interferometric pair is modified as given by:

$$f_{DC} = \frac{f_{DC1} + f_{DC2}}{2}. \tag{2}$$

The Doppler centroids of forward- and backward-looking images for a image are defined by:

$$f_{DC,f} = f_{DC} + n\frac{PBW}{2} \text{ and}$$

$$f_{DC,b} = f_{DC} - n\frac{PBW}{2}, \tag{3}$$

where PBW is Doppler pulse bandwidth.

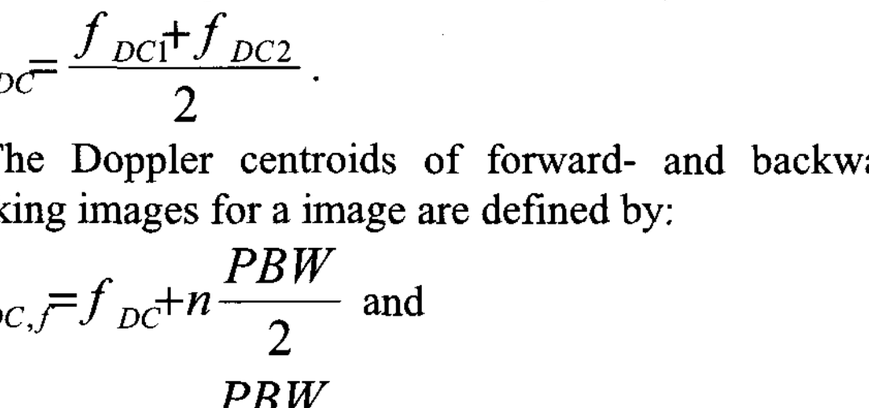

Figure 1. The relationship between PBW (pulse bandwidth) and PBWe (effective pulse bandwidth). If the difference of Doppler centroids between master and slave images is large, PBWe becomes small.

The bandwidths of forward- and backward- looking images must not be overlaid, so that they are defined as given by:

$$\left| f - f_{DC,f} \right| \le (1 - n')\frac{PBWe}{2} \text{ and}$$

$$\left| f - f_{DC,b} \right| \le (1 - n')\frac{PBWe}{2}, \tag{4}$$

where f is Doppler frequency, PBWe is the effective pulse bandwidth, and n' is the modified version of n, which is defined as given by:

$$n' = \frac{PBW}{PBW_e} n \tag{5}$$

Figure 2 represents the change of bandwidth with respect to n or n'.

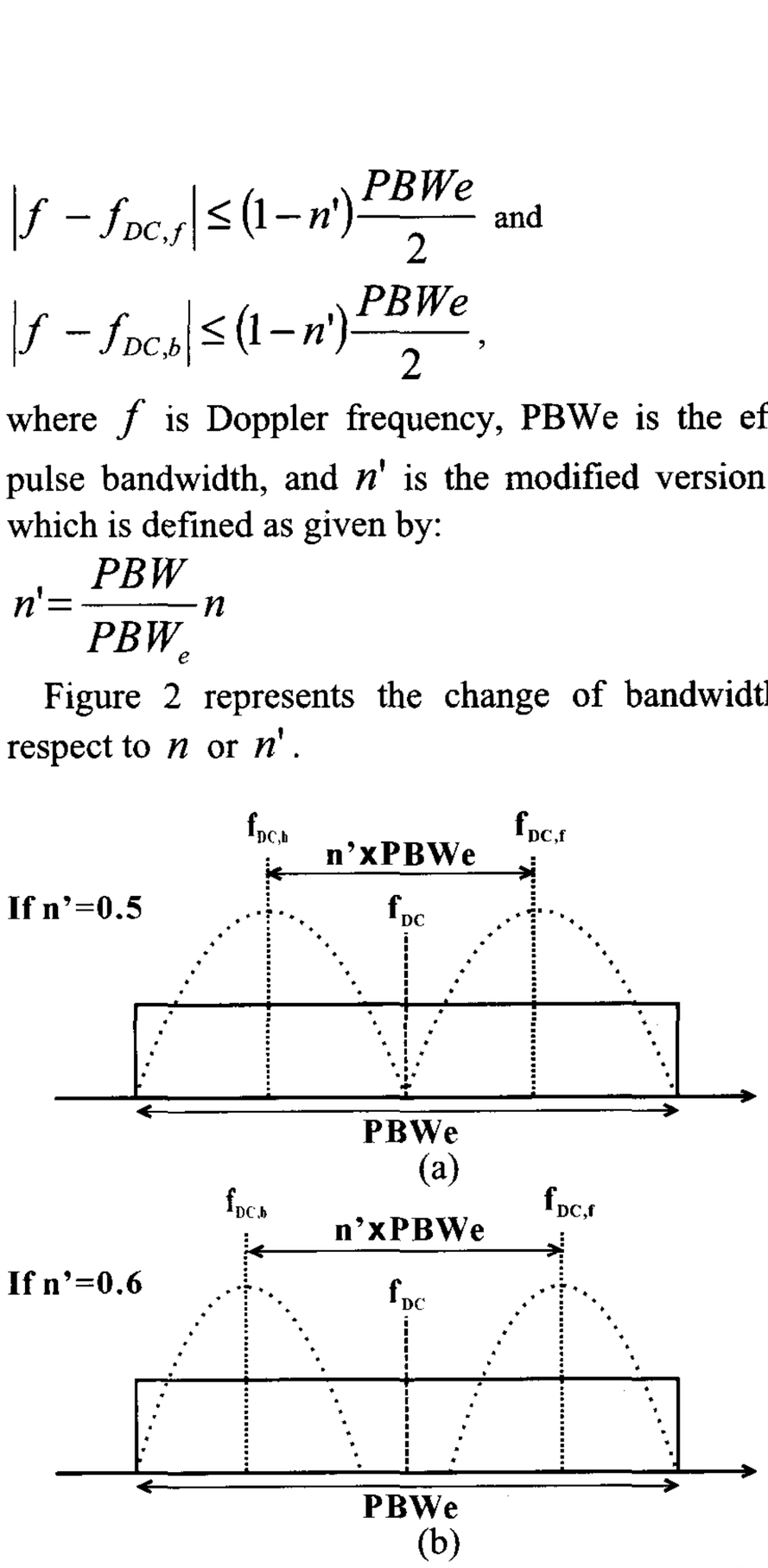

Figure 2. The bandwidth for forward- and backward- looking images when n' is (a) 0.5 and (b) 0.6.

The forward- and backward- looking images are processed using the Doppler centroids and bandwidth of equations (3) and (4), and applied the same range migration correction as seen in Figure 3.

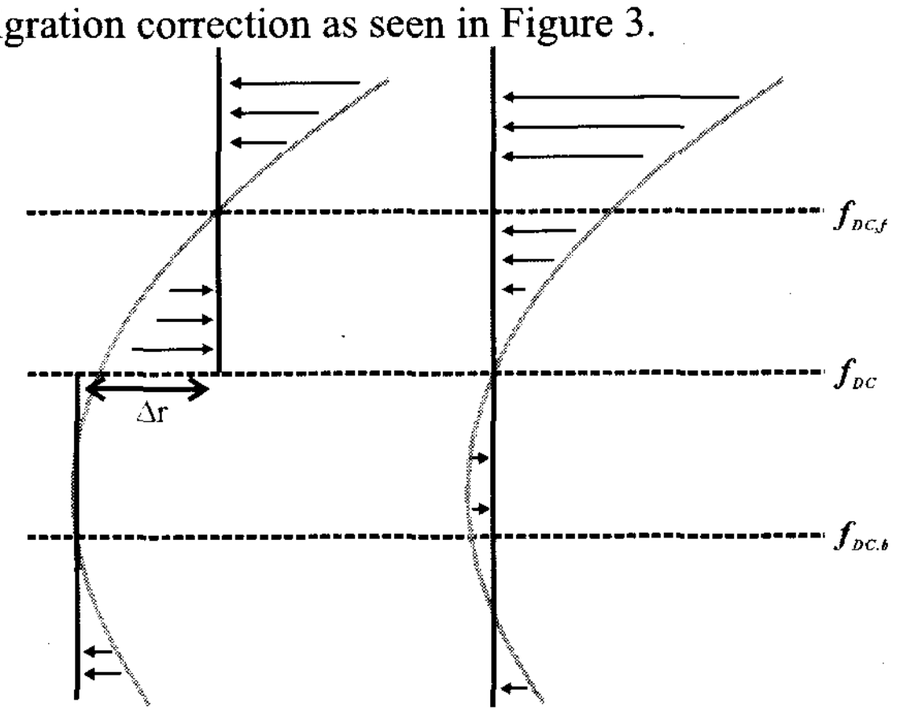

Figure 3. The range migration correction for forward- and backward- looking images. (a) The range migration is corrected by $f_{DC,f}$ and $f_{DC,b}$ and (b) f_{DC}. The forward- and backward looking images have the same range offset because the range migration is corrected by the same Doppler centroid.

Although forward- and backward-looking images have the same range position because of the same range migration correction, their azimuth position is still different, which is caused by different Doppler centroids. The co-registration of backward-looking image with forward-looking image is performed using time shift property of Fourier transform. The azimuth pixel shift (n_{az}) of backward-looking image is defined by:

$$n_{az} = \Delta t \cdot PRF , \tag{6}$$

where PRF is pulse repetition frequency and Δt is azimuth time shift as given by:

$$\Delta t = \frac{\Delta f_{DC}}{f_R} = \frac{f_{DC,b} - f_{DC,f}}{f_R} , \tag{7}$$

where f_R is Doppler rate.

The forward- and backward- images of master and slave images are co-registered using the same range migration correction and time shift property of Fourier transform.

2.3 MAI processing

The forward- and backward- looking interferograms are generated from forward- and backward- images of master and slave images, respectively. To remove azimuth flat earth and topographic phases, forward- and backward- differential interferograms are produced. A complex multilook operation has been carried out on forward- and backward- DInSAR products, and an adaptive filtering is applied to them. MAI is generated from forward- and backward- DInSAR products.

3. APPLICATION

We applied the proposed method to InSAR analysis of the Mw 7.1 1999 California, Hector Mine earthquake to compare with the result reported by Bechor and Zebker (2006). We used two interferogram pairs. The one is the descending orbits of September 15, 1999 and October 20, 1999, both acquired by the ERS-2 satellite, with perpendicular baseline of 21 m, and the other is the descending orbits of January 10, 1993 (ERS-1) and January 8, 1997 (ERS-2) with perpendicular baseline of 12m. Figure 4 represents forward- and backward- images of September 15, 1999. The forward- and backward- images have the same position, because they are generated by the same range migration correction and time shift property of Fourier transform in azimuth compression. We generated forward-looking interferogram from forward-looking images of master and slave images, and backward-looking one from those. These interferograms were used for generating forward- and backward- DInSAR products. Figure 5 shows forward- and backward- differential interferograms generated by applying conventional DInSAR technique to the first interferogram pair.

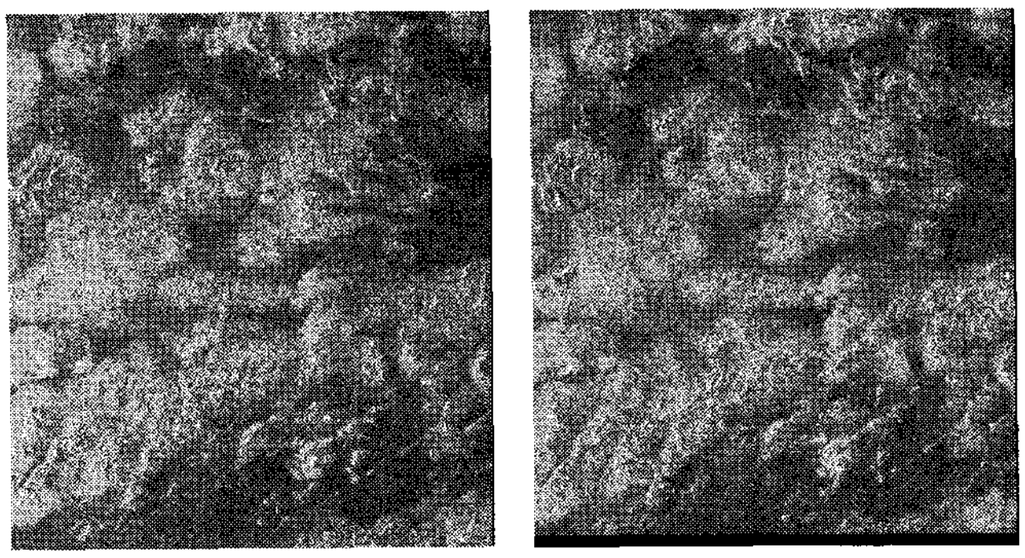

(a) (b)

Figure 4. Forward- and backward- images acquired by ERS-2 satellite on September 15, 1999.

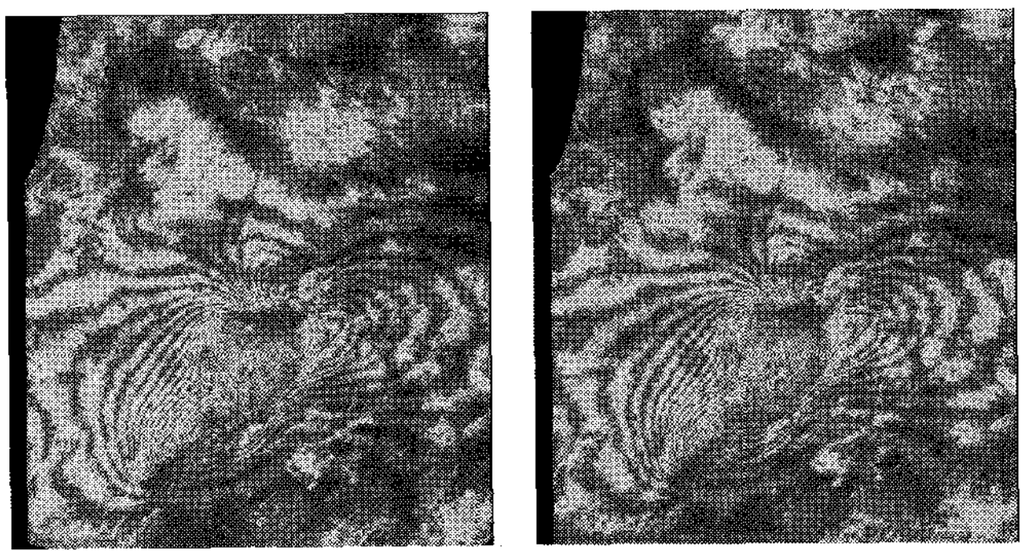

(a) (b)

Figure 5. Forward- and backward- DInSAR products generated by interferogram pair of September 15, 1999 and October 20, 1999.

A complex multilook operation has been carried out on DInSAR products with two look in the range direction and ten in the azimuth one, and adaptive filtering with filtering function based on local fringe spectrum proposed by Goldstein and Werner (1998) has been applied to them.

Figure 6 shows MAI generated from two interferogram pairs. Figure 6 (a) shows MAI produced by the first interferogram pair. This MAI has along-track deformation because of using interferogram pair acquired by images before and after Hector Mine earthquake. However, MAI generated by images before Hector Mine earthquake has not along-track deformation as seen by figure 6 (b).

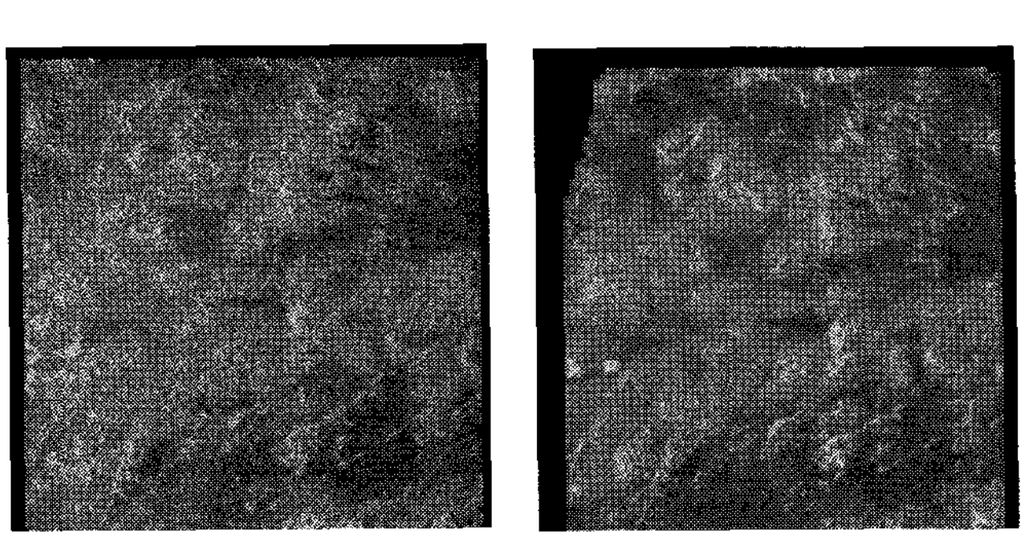

(a) (b)

Figure 6. MAI generated by (a) interferogram pair of September 15, 1999 and October 20, 1999 and (b) interferogram pair of January 10, 1993 and January 8, 1997.

4. DISCUSSION AND CONCLUSION

In this paper, an efficient and robust method is proposed to generate MAI from interferometric pair having non-zero Doppler centroid. We tested the proposed method using ERS images of the Mw 7.1 1999 California, Hector Mine Earthquake. The result shows that the proposed method improved the coherence of MAI and generalized MAI processing algorithm.

REFERENCES

Bechor, N. B. D. and Zebker, H. A., 2006. Measuring two-dimensional movements using a single InSAR pair. *Geophysical Research Letters*, 33, L16311, doi:10.1029/2006GL026883.

Fialko, Y., 2004. Probing the mechanical properties of seismically active crust with space geodesy: Study of the coseismic deformation due to the 1992 Mw 7.3 Landers (southern California) earthquake, *Journal of Geophysical Research*, 109, B03307, doi:10.1029/2003JB002756.

Fialko, Y., Sandwell, D., Simons, M., and Rosen, P., 2005. Three dimensional deformation caused by the Bam, Iran, earthquake and the origin of the shallow slip deficit, *Nature*, 435, pp. 295-299.

Froger, J. L., Fukushimana, Y., Briole, P., Staudachr, T., Souriot, T., and Villneuve, N., 2004. The deformation field of the August 2003 eruption at Piton de la Fournaise, Reunion Island, mapped by ASAR interferometry, *Geophysical Research Letter*, 31, L14601, doi:10.1029/2004GL020479.

Goldstein, R. M. and Werner, C. L., 1998. Radar Interferogram Filtering for Geophysical Applications, *Geophysical Research Letters*, 25(21), pp. 4035-4038.

Jonsson, S., Zebker, H., Segall, P., and Amelung, F., 2002. Fault slip distribution of the M w 7.1 Hector Mine, California, earthquake, estimated from satellite radar and GPS measurements, *Bulletin of the Seismological Society of America*, 92(4), pp. 1377-1389.